ISSN 2176-5480

22nd International Congress of Mechanical Engineering (COBEM 2013)
November 3-7, 2013, Ribeirão Preto, SP, Brazil

COMPARISONS BETWEEN MODELING AND CONTROL METHOD APPLIED TO AN ATOMIC FORCE MICROSCOPE

Ricardo Nozaki
Universidade de São Paulo – Av. Trabalhador São-carlense, 400, Pq Arnold Schimidt
São Carlos - SP/Brasil, CEP 13566-590
ricardonozaki@usp.br

José Manoel Balthazar
Universidade Estadual Paulista "Julio de Mesquita Filho" - Av. Vinte e Quatro A, 1515
Rio Claro – SP/Brasil, CEP 13500-230
jmbaltha@rc.unesp.br

Angelo Marcelo Tusset
Utfpr – Av Monteiro Lobato, s/n - Km 04
Ponta Grossa – PR/Brasil, CEP 84016-210
a.m.tusseet@gmail.com

Atila Madureira Bueno
Utfpr – Av Monteiro Lobato, s/n - Km 04
Ponta Grossa – PR/Brasil, CEP 84016-210
atilabueno@utfpr.edu.br

Bento Rodrigues Pontes Jr.
Universidade Estadual Paulista "Julio de Mesquita Filho" - Av. Eng. Luiz Edmundo C. Coube 14-01
Bairro: Vargem Limpa - Bauru – SP/Brasil, CEP 17033-360
brpontes@feb.unesp.br

Helio Aparecido Navarro
Universidade de São Paulo – Av. Trabalhador São-carlense, 400, Pq Arnold Schimidt
São Carlos - SP/Brasil, CEP 13566-590
han@sc.usp.br

Abstract. *This article portrays the study of an atomic force microscope, in a non-contact mode, from analytical, numerical, mathematical, experimental modeling to control. The analysis of the model is made according classical models in the literature and a model was obtained through experiments with AFM to test the efficiency of the Linear Optimal Control being applied to control and suppress the chaotic motion present in the atomic force microscope. Comparison between a classical model and an experimental model is made through the simulation results that are presented with an aim to identify the advantages, disadvantages, possible errors of modeling and one matrix uncertainties like capillary forces, noises or a small force due to air resistance between tip- surface.*

Keywords: *Modeling, Chaos, AFM, Control.*

1. INTRODUCTION

The Scanning Tunneling Microscope (STM) and the Atomic Force Microscope, both invented by G. Binnig, are the most powerful tools to perform the surface investigation (Binnig and Gerber, 1986). Instead of showing or using different models, from the literature that characterize the dynamics of the AFM's cantilever, here is trying to acquire a model using raw data obtained from the AFM's calibration, such as tensile strength, deflections, forces between tip-distance surface, springer constant, damping, amplitude, frequency, vibration velocity, acceleration, q factor and mass of cantilever. In the AFM system a microcantilever identifies the surface that is being investigated, bending upwards or downwards according to the topography (Bueno, A.M., 2012).These deflections are caused by forces, acting between the probe and the sample. The different techniques provide several opportunities to take pictures of different types of samples and to generate a wide range of information. The methods of making images, also called scanning or modes of operation, mainly refer to the distance maintained between the probe end (which we call tip) and the sample at the time of scanning, as well as the ways to move the tip over the surface to be studied. The detection of the surface is carried out aiming at the creation of its image.

There is a continuum of possible ways of making images, due to different interactions depending on the distance between the tip and the sample, as well as the detection scheme used. The choice of the appropriate mode depends on

ISSN 2176-5480

the specific application. When the tip approaches the sample it is first attracted towards the surface, due to a wide range of attractive forces in the region, as the van der Waals forces.

This attraction increases until the tip is very close to the sample, the atoms of both are so close that their electronic orbits begin to repel. This electrostatic repulsion weakens the attractive force over distance. The force is void, when the distance between atoms is about a few angstroms (about the characteristic distance of a chemical bond). When the forces become positive, we can say that the atoms of the tip and sample are in contact and repulsive forces eventually dominate.

The AFM system has become a popular and useful instrument to measure the intermolecular forces, with atomic-resolution, that can be applied in electronics, biological analysis, materials, semiconductors etc. The AFM systems may experience undesirable and unexpected behavior and instability, due to the effects of nonlinearities of the systems. Many kinds of control methods aiming to decrease or eliminate the effects of the nonlinearities that have been studied see Hornstein et. al (2008) and Yabuno (1999).

Through an atomic force microscope was built the force-distance curves that can easily visualize the three operating modes of the AFM (non-contact mode, tapping mode, contact mode). For this realization was used three kinds of microcantilevers (two rectangular and one triangular) and the microscope is not remained in constant amplitude, causing a difference in tip-sample size. Classical AFM models have this factor in Van der Waals equation and even without this approach it is possible to do a regression to a system of differential equations and thus find approximately the values of damping, non-linear springer, and others using raw data file of the AFM, normal linear spring, cantilever's mass, others capillary forces, displacement of cantilevers, deflections, velocities of cantilevers, Q factor, and natural frequency.

The method to obtain the normal spring is credited by Sadder et. Al. (1999) and was calculated from the length and width of the microcantilever measured in the optical microscope, using the factor q, and the resonance frequency. The microcantilever's mass is obtained by its density, making mass divided by volume.

The method of phase space reconstruction are derivative coordinates of which Packard et al. (1980) is used:

$$\dot{S}(t) \approx \frac{S[t_0 + (n+1)\Delta t] - S(t_0 + n\Delta t)}{\Delta t}$$

n=1,2,3,…,512 samples and Δt=1/12.5 seconds

In final session is reserved to Numerical simulations are used in order to analyze the efficiency of the control technique applied to the AFM system. However, due to simplifications and inappropriateness of the system and simulation models, to uncertainties in the system parameters and to dynamic instabilities, the simulation results may present errors. In order to improve the simulation results, uncertainty analysis is used.

In this article we study the case where the system has a chaotic behavior, using the mathematical model of AFM proposed by Jalili et. al (2004), Hornstein et. al (2008) and Wang et al. (2009). With the goal of suppression of chaotic behavior it will be considered two control techniques, the Optimal Linear Feedback control proposed by Rafikov and Balthazar (2008).

The paper is organized as follows: Section 2 begins with non-linear model of the AFM system, the parameters being determined to create chaos, using perturbation methods we obtain an analytical solution. Section 3 describes the application of the application of the optimal linear control and its approximation and validation with a simulation of real AFM. In Section 4 we present the acknowledgements. In Section 5, we present the concluding remarks.

2. AFM CONSTITUTIVE MODELING

It is well known that the nonlinear dynamics of the AFM is an emerging topic of research in Engineering Sciences, since its discovering by Binnig and Quate (1986), and according to a number of authors such as Jalili et. al (2004), Garcia et. al (2000), Raman et. al (2008) and Lozano et. al (2008) presenting the mathematical models that govern the dynamics of AFM cantilevers.

According to Jalili et. al (2004) and Wang et. al (2009) a mathematical model to a cantilever-sample interaction of an AFM process, may be presented as shown in Fig. 1. The cantilever is taken as a single spring-mass system, with a spring constant *k* and equivalent mass *m*.

ISSN 2176-5480

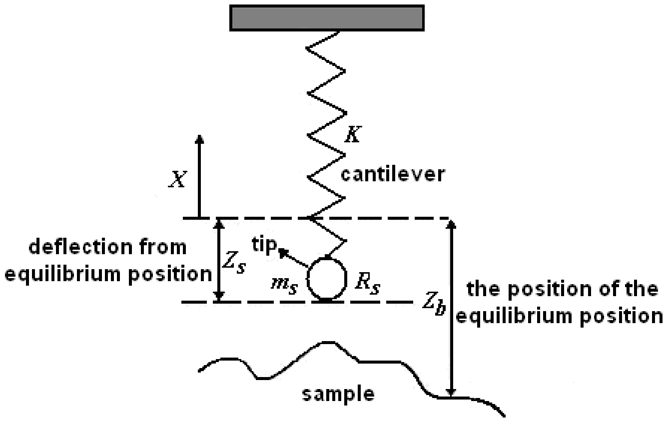

Fig. 1. AFM Model of Sinha (2005)

2.1 Modeling the AFM

The cantilever interacts with the sample, via a sharp tip, which is mounted on the cantilever. The cantilever–tip–sample system is mathematically modeled by a sphere of radius R_s and mass m_s suspended by a spring of stiffness: $k = k_{l_s} + k_{nl_s}$. We will frequently refer to the mass m_s, as being the tip of the cantilever. Van der Waals forces denotes the attraction/repulsion force (i.e., the interaction forces), between the sphere and sample surface.
Thus, the potential for the tip–sample assembly is given by:

$$P = -\frac{A_c R_c}{6(Z_b + X)} + \frac{1}{2}k_{l_s} X^2 + \frac{1}{4}k_{nl_s} X^4 \qquad (1)$$

The net energy of the system due to the mass m_s (tip-sample interaction) of the cantilever is given by E:

$$E = \frac{1}{2}\dot{X}^2 + \frac{1}{2}\omega_1^2 X^2 + \frac{1}{4}\omega_2^2 X^4 - \frac{D\omega_1^2}{(Z_b + X)} \qquad (2)$$

where: k_{l_s} is the linear stiffness, k_{nl_s} is the nonlinear cubic stiffness, $\omega_1 = \sqrt{\frac{k_{l_s}}{m_s}}$ is the first-order mode frequency, $\omega_2 = \sqrt{\frac{k_{nl_s}}{m_s}}$ and $D = \frac{A_c R_c}{6k_{l_s}}$, where D is the molecular diameter, A_c is a Hamaker constant, R_c is the cantilever-tip radius and Z_b is the distance from the fixed coordinate frame to the sample. Typical values that are found in AFM application are $R_c = 150$ nm, $A_c = 10^{-19}$ J, $\omega_1 = 74166.72 \ rad/s$ and $k_{l_s} = 0.0167$ N/m [6, 22]. Considering $X_1 = X$ and $X_2 = \dot{X}$. The dynamics of the tip-sample system derived from the above governing equations of motion is given below:

$$\dot{X}_1 = \frac{\partial E}{\partial X_2}$$
$$\dot{X}_2 = -\frac{\partial E}{\partial X_1} \qquad (3)$$

The nonlinear dynamic system describing the AFM operation in Fig. 1 is obtained based on the model proposed by Payam et. al (2009) including the nonlinear cubic stiffness. Substitute (1) and (2) in (3):

$$\begin{cases} \dot{X}_1 = X_2 \\ \dot{X}_2 = -\omega_1^2 X_1 - \omega_2^2 X_1^3 - \dfrac{D\omega_1^2}{(Z_b + X_1)^2} \end{cases} \tag{4}$$

The beam is forced by a small sinusoidal force, which is given by $f\sin(wt)$, where w is excitation frequency and f is the amplitude of excitation. Considering the sinusoidal force the differential equation system can be written as:

$$\begin{aligned} \dot{X}_1 &= X_2 \\ \dot{X}_2 &= -\omega_1^2 X_1 - \omega_2^2 X_1^3 - \frac{D\omega_1^2}{(Z_b + X_1)^2} + f\sin wt \end{aligned} \tag{5}$$

Or in dimensionless form:

$$\begin{aligned} \dot{x}_1 &= x_2 \\ \dot{x}_2 &= -a_1 x_1 - a_2 x_1^3 - \frac{b}{(z + x_1)^2} + c\sin\tau \end{aligned} \tag{6}$$

where: $\tau = wt$, $x_1 = \dfrac{X_1}{Z_s}$, $z = \dfrac{Z_b}{Z_s}$, $a_1 = \dfrac{\omega_1^2}{w^2}$, $a_2 = \dfrac{\omega_2^2 Z_s^2}{w^2}$, $b = \dfrac{D\omega_1^2}{w^2 Z_s^3}$, and $c = \dfrac{f}{w^2 Z_s}$.

Considering the parameters: $b = 0.02173$, $c = 2.6364$, $z = 2.5$, $a_1 = 0.14668$ and $a_2 = 2.1269$. In Fig. 2, the displacement, the phase portrait diagram, the Lyapunov exponent and the Poincare map for the considered micro-cantilever are shown.

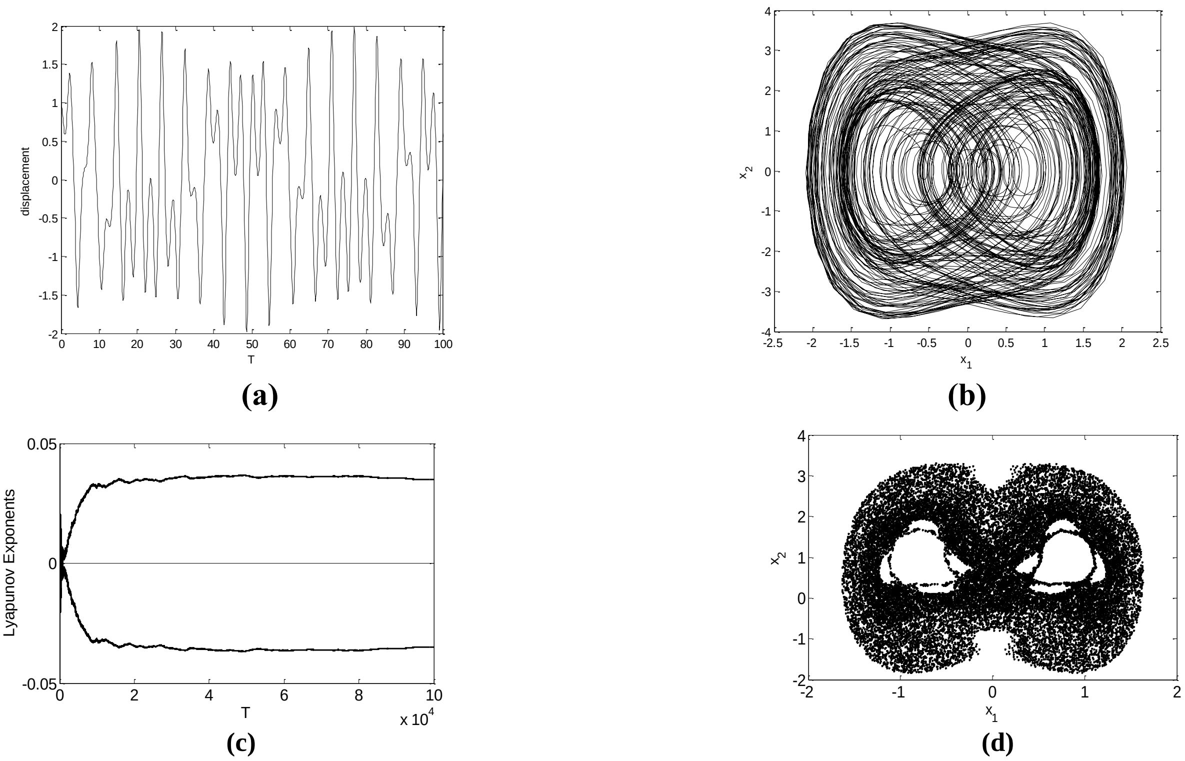

Fig. 2. (a): The displacement of AFM without control. **(b):** Phase portrait of atomic force microscope. **(c):** Exponents of Lyapunov: $\lambda_1 = 0.335$ and $\lambda_2 = -0.035$. **(d):** Poincare map

2.2 Searching of an analytical solution

ISSN 2176-5480

Yabuno (2003) and Raman (2003) wrote the van der Waals force in terms of the Taylor series, justifying the fact that the force is highly nonlinear, considering by approximation, the cubic and quadratic terms, as linear and constant, help the study of the adopted mathematical model, applying the theory of perturbation techniques and the analysis of the parameters of damping, as well as the elastic constant of the cubic and quadratic terms are easier to handle. In this work the nonlinear term $-\frac{b}{(z+x_1)^2}$ is expanded in a Taylor series at the point $x_1 = x_{st} = -0.0239$, critical point of:

$$a_1 x_{st} + a_2 x_{st}^3 + \frac{b}{(z+x_{st})^2} = 0.$$

$$-\frac{b}{(z+x_1)^2} = -0.00347 + 0.00278x_1 - \\ -0.00167x_1^2 + 0.00093x_1^3 \tag{7}$$

And replacing (7) into (6):

$$\begin{aligned} x_1' &= x_2 \\ x_2' &= -L - Jx_1 - Ix_1^2 - Hx_1^3 + c\sin\tau \end{aligned} \tag{8}$$

where: $L = 0.00347$, $J = 0.1439$, $I = 0.00167$, $H = 2.1260$ and $c = 2.6364$.

2.2.1 Multiple scales method

We use the method of multiple scales to find an approximate analytical solution to the above governing equation; This is done for a balance of order as follows.

$$\mu'' + H\varepsilon^2\mu^3 + I\varepsilon\mu^2 + J\mu + \varepsilon^2 L - c\varepsilon^2 \sin wt = 0 \tag{9}$$

Where $\mu = x$ and ε is the parameter responsible for this balance [26]. Introducing the scales $T_0 = \tau$ and $T_1 = \varepsilon\tau$, looking for solutions in the following way:

$$\mu = \mu_0 + \varepsilon\mu_1 + O(\varepsilon^2) \tag{10}$$

with:

$$\begin{aligned} \frac{d}{d\tau} &= D_0 + \varepsilon D_1 + \varepsilon^2 D_2 + \ldots \\ \frac{d^2}{d\tau^2} &= D_0^2 + 2\varepsilon D_0 D_1 + \varepsilon^2 (D_1^2 + 2D_0 D_2) + \ldots \end{aligned} \tag{11}$$

ISSN 2176-5480

Replacing (10) into (9) and considering the derivatives (11), (9) is represented in the perturbed form:

$$\left(D_0+\varepsilon D_1+\varepsilon^2 D_2+\ldots\right)^2\mu+H\varepsilon^2\mu^3+I\varepsilon\mu^2+J\varepsilon\mu+\varepsilon^2 L=c\varepsilon^2\sin wt \tag{12}$$

Resulting:

$$\begin{cases} D_0^2\mu_0+J\mu_0=0 \\ D_0^2\mu_1+J\mu_1=-2D_1D_0\mu_0-I\mu_0^2 \\ D_0^2\mu_2+J\mu_2=-2D_0D_1\mu_0-D_1^2\mu_0^2-2D_0D_1\mu_1-\ldots \\ \ldots-H\mu_0^3-2I\mu_0\mu-L+c\sin wt \end{cases} \tag{13}$$

One possible solution for μ is:

$$\mu=a\cos(\sqrt{J}\tau+\beta)+ \\ +\varepsilon\left(\frac{ka^2}{2}\cos(2\sqrt{J}\tau+2\beta)-\frac{Ia^2}{2}\right) \tag{14}$$

$$\beta=\frac{-\left(4I^2-2Ik-3H\right)a^2\varepsilon\tau}{8J}+\beta_0 \tag{15}$$

Where: $k=\dfrac{-I}{-4J+1}$, β_0 is a constant and a is assumed to be different from zero .

3. Control in AFM

The tip-sample distance must be kept constant by the control system at a pre-defined setpoint. Vertical tip-sample relative motion is then due to topographic changes in the sample surface. The AFM system generates the topographic images, during the scanning process, based on the tip-sample distance feedback signal (Bueno et. al 2012). In this section, we propose stabilization of the chaotic microcantilever oscillations using Optimal Linear Feedback control method and SDRE control method.

3.1 Optimal Linear Feedback Control

We use the method developed by [16] to control the system. This method seeks to find an optimal linear feedback control where they find conditions for the application of linear control technique in the nonlinear system, ensuring the stability of the problem. We remark that, due to the simplicity in configuration and implementation, the linear state feedback control is especially attractive [16, 27]. So far, this control method has been successfully applied to various works including chaos, see [16, 27-32].

3.1.1 Application of optimal linear feedback control

The equations that describe the motion of the system with the control law U are described by the following nonlinear equations:

$$\dot{x}_1 = x_2$$
$$\dot{x}_2 = -a_1 x_1 - a_2 x_1^3 - \frac{b}{(z + x_1)^2} + c\sin\tau + U$$

(16)

With

$$U = \tilde{u}_o + u_{of}$$

(17)

Where u_{of} is the f*eedback* control, and $\tilde{u}_o$ is the feedforward control, for optimal control*,* given by:

$$\tilde{u}_o = \dot{x}_2^* + a_1 x_1^* + a_2 x_1^{*3} + \frac{b}{(z + x_1^*)^2} - c\sin\tau$$

(18)

Where x^* is the desired periodic orbit. Replacing (18) into (16) and defining the deviations from the desired orbit:

$$e = (x - x^*)$$

(19)

We obtain:

$$\dot{e}_1 = e_2$$
$$\dot{e}_2 = -a_1 e_1 - a_2 (e_1 + x_1^*)^3 + a_2 x_1^{*3} - \frac{b}{(z + e_1 + x_1^*)^2} + \frac{b}{(z + x_1^*)^2} + u_{of}$$

(20)

Considering the system (20) written in the following way:

$$\dot{e} = Ae + g(e) - g(x^*) + Bu_{of}$$

(21)

where:

$$e = \begin{bmatrix} e_1 \\ e_2 \end{bmatrix},\ A = \begin{bmatrix} 0 & 1 \\ -a_1 & 0 \end{bmatrix},\ B = \begin{bmatrix} 0 \\ 1 \end{bmatrix} \text{ and}$$

$$g(e) - g(x^*) = G(e, x^*) =$$
$$= \begin{bmatrix} 0 \\ -a_2 (e_1 + x_1^*)^3 + a_2 x_1^{*3} - \dfrac{b}{(z + e_1 + x_1^*)^2} + \dfrac{b}{(z + x_1^*)^2} \end{bmatrix}.$$

According to [27], if there are an error weighted matrix Q, and the control weighted matrix R, positive definite symmetric matrix, and a matrix Riccati P, such that the matrix:

$$\tilde{Q} = Q - G^T(e, x^*)P - PG(e, x^*)$$

(22)

is positive definite matrix G restricted, then the control u_{of} is optimal and transfers the non-linear systems from any initial state, to the final state:

$$e(\infty) = 0 \tag{23}$$

minimizing the functional:

$$J = \int_0^{\infty} (e^T \tilde{Q} e + u_{of}{}^T R u_{of}) dt \tag{24}$$

Then control u_{0f} can be found by solving the equation:

$$u_{of} = -R^{-1} B^T P e \tag{25}$$

Since the symmetric matrix P, can be obtained from the Riccati algebraic equation

$$PA + A^T P - PBR^{-1} B^T P + Q = 0 \tag{26}$$

The matrix A and B have the following form:

$A = \begin{bmatrix} 0 & 1 \\ -0.14668 & 0 \end{bmatrix}$ and $B = \begin{bmatrix} 0 \\ 1 \end{bmatrix}$.

Choosing:

$Q = \begin{bmatrix} 250 & 0 \\ 0 & 20 \end{bmatrix}$ and $R = [0.1]$.

and using the command LQR from Matlab[r], we get:

$P = \begin{bmatrix} 86.5602 & 4.9853 \\ 4.9853 & 1.7312 \end{bmatrix}$ and $K = [49.8535 \quad 17.3120]$.

Then replacing them, into (25) the control is given by:

$$u_{of} = -49.8535 e_1 - 17.3120 e_2 \tag{27}$$

Finally, we can conclude that the optimal function u_{of} has the following form:

$$u_{of} = -49.8535(x_1 - x_1^*) - 17.3120(x_2 - x_2^*) \tag{28}$$

For the optimal control verification (27), the function (22) is numerically calculated with $L(\tau) = e^T \tilde{Q} e$, if $L(\tau)$, resulting to be defined positive. It is the sufficient standard to assure that the control (27), obtained with the use of the matrixes Q and R, will be optimal, and $\tilde{Q}$ is defined positive. The next figure shows the trajectory of the periodic

ISSN 2176-5480

function, considering the application of control, and the desired orbit (x_1^*) the equation (15).

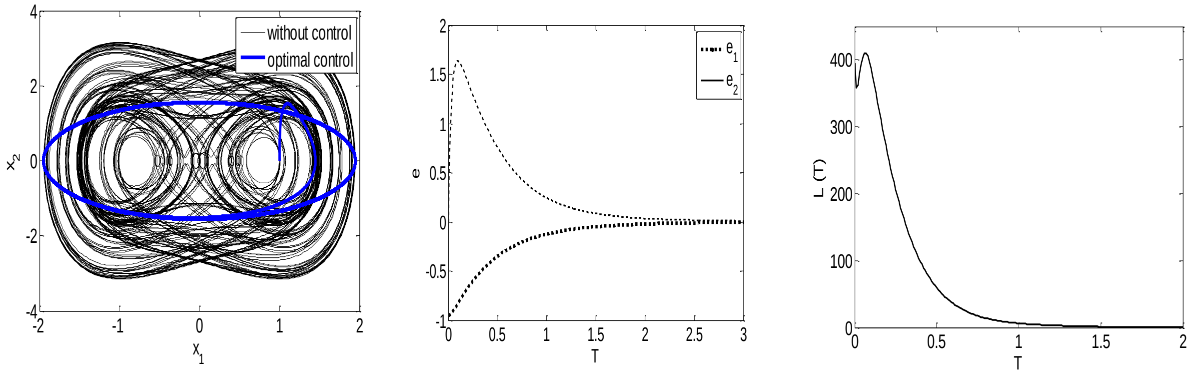

(a) **(b)** **(c)**

Fig. 2. (a): Phase portrait, chaotic (black) and controlled orbit (blue) **(b):** Signal deviations **(c):** $L(t)$ calculated in optimal trajectory

In Fig. 3, it can be seen that the control was effective to move the system from a chaotic state to a periodic orbit (15), using feedback control (28) just enough to take periodic orbit. Also, we can see in Fig. 3.f, the control signal used by the feedforward control (18) to keep the system in the desired orbit, we should consider this as a reference signal to move.

3.2 Modeling experimental AFM

The experimental work was performed with a Veeco afm® and obtained raw data file to perform via matlab the force curve. Matrix of deflections, z displacements in time, signals piezo, z piezo , q factor, frequency was collected to make a nonlinear regression, finding an equation to analyze each variable and its influence, visualized in the phase portrait modeled more next to real.

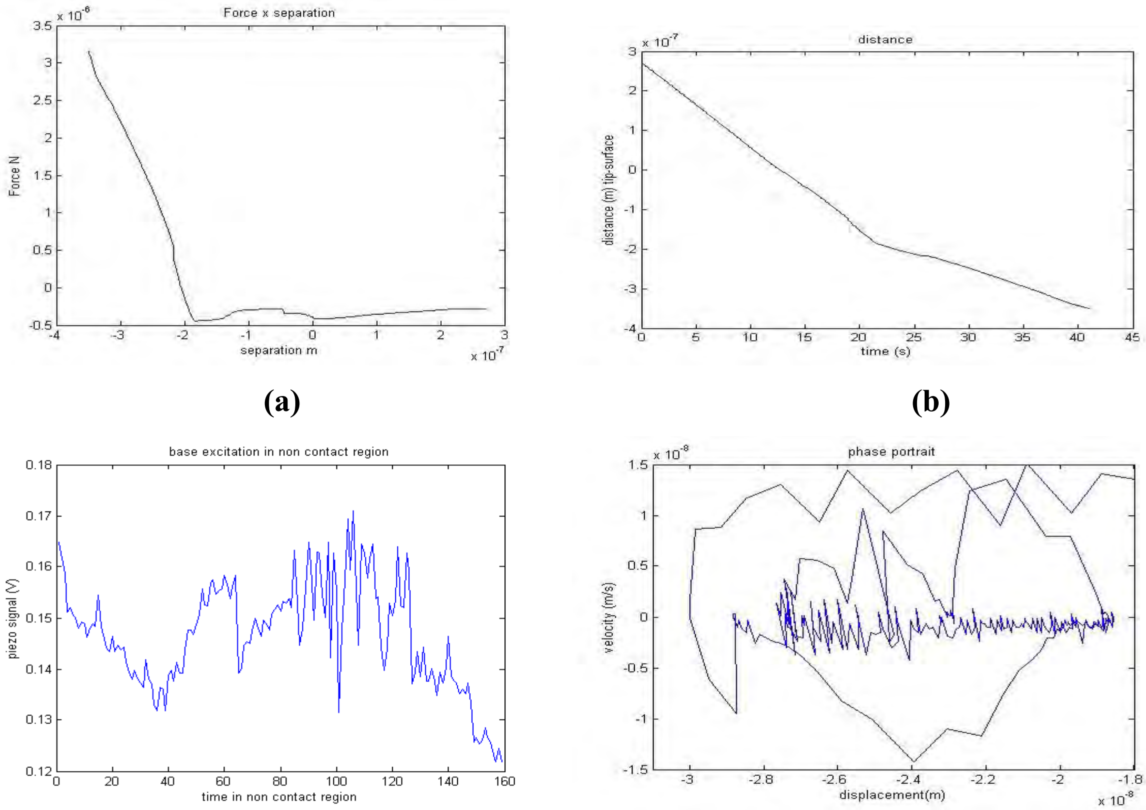

(a) **(b)**

(c) **(d)**

ISSN 2176-5480

Fig.3. (a): Tip-surface distance versus force, calculated through multiplication of K by deflections, **(b)** distance tip-surface in time which shows the distance between tip surface positive to negative space, **(c)** base excitation from piezo signal (V), **(d)** Phase portrait of experimental data

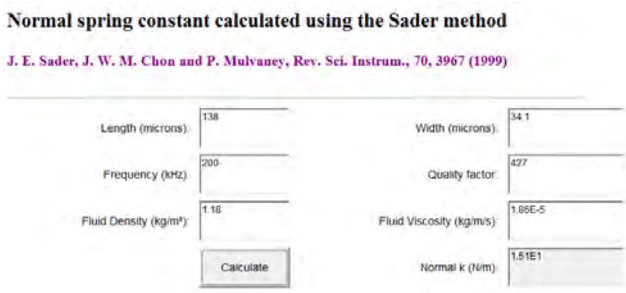

Fig 4. On line Sader Method

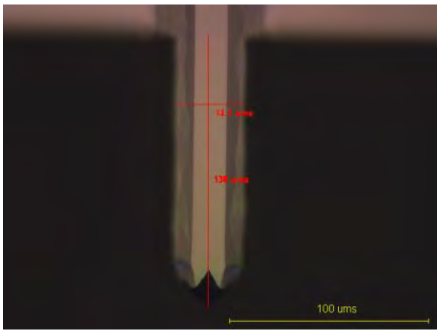

Fig 5. Dimension's Cantilever AFM

The regresssion is made to obtain the equations for the dynamics AFM. It was chosen the method of nonlinear regression lsqnonlin and found the cubic term k³, damping (C), and the distance of tip-surface was studied which determine major or minor interaction tip surface. There many possible to make the regression and the first step is to analyze the equation to begin the regression.

$$\mathbf{M}\ddot{\mathbf{x}}(t)+\mathbf{C}\dot{\mathbf{x}}(t)+\mathbf{K}\mathbf{x}(t)+\mathbf{K}^3\mathbf{x}(t)=\mathbf{f}(t) \tag{29}$$

$$\mathbf{M}\ddot{\mathbf{x}}(t)++\mathbf{K}\mathbf{x}(t)+\mathbf{K}^3\mathbf{x}(t)=\mathbf{f}(t) \tag{30}$$

$$\mathbf{M}\ddot{\mathbf{x}}(t)+\mathbf{C}\dot{\mathbf{x}}(t)+\mathbf{K}\mathbf{x}(t)=\mathbf{f}(t) \tag{31}$$

$$\mathbf{M}\ddot{\mathbf{x}}(t)+U_{ncertainty}+\mathbf{K}\mathbf{x}(t)+\mathbf{K}^3\mathbf{x}(t)=\mathbf{f}(t) \tag{40}$$

The results to the equation have a better convergence to the true and there is a smaller error shown in equation (40). The error close to zero would be the ideal characteristics of the actual model to the equation, but we know that there are other forces acting in the equation. The error (in Newtons) is an uncertainty, with chances of it being a small force due to air resistance. **M** is the mass, $\ddot{\mathbf{x}}(t)$ is the matrix of cantilever velocities, U is matrix of uncertainties, K is the Normal spring constant, K³ is the non linear spring, **x**(t) is the cantilever deflections and the **f**(t) is the Van der Waals force and the base excitation. When U(t) is near from zero, it would show how much the model is near to real model. The numerical study dimensionless of AFM experimental model compared with AFM model (6) is:

$$\dot{x}_1 = x_2$$

$$\dot{x}_2 = -a_1x_1 - a_2x_1^3 - \frac{b}{(d\cos(wt)z + x_1)^2} + c\sin\tau + U_{ncerntainty}$$

where: $\tau = wt$, $x_1 = \dfrac{X_1}{Z_s}$, $z = \dfrac{Z_b}{Z_s}$, $a_1 = \dfrac{\omega_1^2}{w^2}$, $a_2 = \dfrac{\omega_2^2 Z_s^2}{w^2}$, $b = \dfrac{D\omega_1^2}{w^2 Z_s^3}$, and $c = \dfrac{f}{w^2 Z_s}$.

The big problem in the modeling from real to equation is the way it was acquired matrices, when distance tip- surface size isn't keeping the constant amplitude. The tip moves down toward the sample and slope. The matrix of piezo signal is an approach of sinusoid signal, Z_s is the position of matrix deflection which occurs contact. The alteration stays to distance z which is represent in form of $d\cos(wt)z$. This is the most real representation possible and the variables obtained is showed as follow:

3.3 Table 1. The following table shows some properties obtained in experiments and numerically via Matlab®.

Cantilever Properties/Parameters/Variables	unit	Method of discovery	Citation/proceedings/formula

ISSN 2176-5480

Normal Spring constant (κ_1)	N/m	Sadder Method	http://www.ampc.ms.unimelb.edu.au/afm/calibration.html
Dumping (c)	N.m/s	Lsqnonlin	Matlab® comand
Hamaker constant (H)	Joule	literature	$A = \pi^2 C\rho_1\rho_2$
Non linear Spring (κ_2)	N/m³	Lsqnonlin	Matlab® comand
Velocity ($x(2)$)	nm/s	calculated	Packard(1980)and Takens(1981)
Deflection ($x(1)$)	nm	Raw data afm	Conversion by sensitivy
Aceleration ($\dot{x}(2)$)	nm/s^2	calculated	Packard(1980) and Takens(1981)
Cantilever's mass (m)	g	Material Density	V=m/d
Amplitude (due piezo) (A)	V	Raw data afm	-
Sensitivy (S)	nm/V	Tan force curve	Matlab® comand
Z cantilever position (z)	nm	Raw data afm	-
Z piezo position (zp)	nm	Raw data afm	-
Time (t)	s	Regulator	-
Pixels (pix)	-	512 points	-
Material surface (mat)	-	-	Silicon
Cantilever's material		Cantilever's Manual	SI_3N_4
Q factor (Q)	-	Afm information	-
Drive frequency (df)	Hz	Raw data afm	-
Phase (ph)	-	Raw data afm	-
Cantilever's Width (cw)	nm	Optical microscopy	-
Cantilever's Height (ch)	nm	Optical microscopy	-
Tip's Ratio (R)	nm	Optical microscopy	-
Natural Frequency (w_0)	Hz	Calculated	-
Force (F)	nN	Calculated	F=kx(1)

3.4 Simulations of experimental AFM model.

The equation was work in dimensionless form and was obtained:

$$a_1 = 0.1015, a_2 = 7.091223092993430e^{-17}, b = 6.212e^{-2}, z = 0.102, k = 15.1,$$

$$m = 3.10^{-10}, \omega = \sqrt{\frac{k}{m}}, d = d(t) = 0.9 + 0.000001.t, U(t) = rand(V)$$

With U(t) a matrix of very small elements of force.(around 10^{-10})

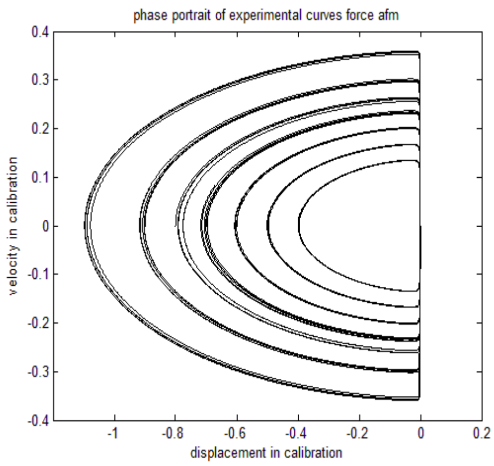

(a)

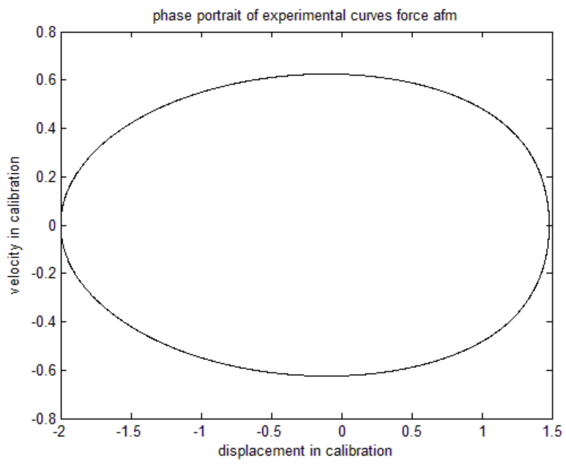

(b)

Fig. 6(a) is the phase portrait with various initial conditions and a new formulation for z parameter . **6(b)** is the phase portrait with parameter z in form constant equal a 2. In both cases the AFM oscilator stays in periodic orbit and the fig(b) is a real case that is aproach a AFM oscilator controled by optimal linear control.

ISSN 2176-5480

4. CONCLUSIONS

Using computer simulations we have shown that for certain parameters the AFM system exhibits chaotic behavior. In order to suppress the chaotic behavior, keeping the system in a periodic orbit, were compared two AFM system, formulations, analysis, nonlinear phenomena, and control strategy.

Analyzing the Figs. 2(a) and 6(b), we conclude that control technique is effective in controlling the system for special conditions, and the Optimal Linear Feedback bring the system to the periodic.

5. ACKNOWLEDGEMENTS

"We are grateful to the "Laboratório de Filmes Finos do Instituto de Física da Universidade de São Paulo", Brazil, for the SPM facility (FAPESP proc.# 95/5651-0)".

The authors acknowledge CNPq (Conselho Nacional de Desenvolvimento Científico) and FAPESP (Fundação de Amparo à Pesquisa do estado de São Paulo) and CAPES (Coordenação de Aperfeiçoamento de Pessoal de nível Súperior).

6. REFERENCES

Arbex, H. C., Balthazar, J.M., Pontes, B.R., Brasil, R. M. L. R. F., TUSSET, A. M.. *Dinâmica Não-linear e controle de um sistema vibratório do tipo Maglev, excitado por um motor não ideal.* Em: CONEM, 2012, São Luiz, Maranhão

Ashhab, M., Salapaka M.V., Dahleh M., Mezic H I. *Dynamical analysis and control of microcantilevers*. Automatica; 1999, 35: pp. 1663-1670.

Banks, HT, Lewis BM, Tran HT. *Nonlinear feedback controllers and compensators: a state-dependent Riccati equation approach*. Comput. Optim. Appl.; 2007; 37: pp.177-218.

Binnig, G., Gerber C., Quate C. *Atomic Force Microscope*. Phys. Rev. Lett.; 1986; 56: pp. 930-933.

Bueno, AM., Balthazar, JM., Piqueira, JRC. *Phase-Locked loops lock-in range in Frequency Modulated-Atomic Force Microscope nonlinear control system*. Communications in Nonlinear Science & Numerical Simulation; 2012; 17: pp. 3101-3111.

Fang, Y, Feemster MG., Dawson DM., *Jalili N. Nonlinear Control Technicolor for the Atomic Force Microscope System*. Proceedings of IMECE2002 ASME International Mechanical Engineering Congress & Exposition November 17.22; 2002, New Orleans, Louisiana.

Godoy, W. R., Balthazar, J. M., Pontes, B. R., Felix, J. L., Tusset, A. M.. *A note on non-linear phenomena in a non-ideal oscillator, with a snap-through truss absorber, including parameter uncertainties*. Proceedings of the Institution of Mechanical Engineers, Part K: Journal of Multi-body Dynamics, v. 227, p. 76-86, 2013

Hornstein, S, Gottlieb O. *Nonlinear dynamics, stability and control of the scan process in noncontacting atomic force microscopy.* Nonlinear Dyn.; 2008; 54: pp. 93-122.

Hornstein, S., Gottlieb O. *Nonlinear dynamics, stability and control of the scan process in noncontacting atomic force microscopy*. Nonlinear Dyn.; 2008; 54: pp. 93-122.

Jalili, N, Laxminarayana K. *A review of atomic force microscopy imaging systems: application to molecular metrology and biological sciences*. Mechatronics; 2004; 14: pp. 907-945.

Jayaram, A., Tadi M. *Synchronization of chaotic systems based on SDRE method. Chaos, Solitons & Fractals*, 2006; 28(3): pp. 707-715.

Lozano, JR, Garcia R. Theory of Multifrequency Atomic Force Microscopy. Physical Review Letters; 2008; PRL 100: 076102.

Misra, S., Dankowicz H., Paul M.R. *Event-driven feedback tracking and control of tapping-mode atomic force microscopy*. Proc. R. Soc. A; 2007.

Mracek, PC, Cloutier JR. *Control designs for the nonlinear benchmark problem via the state-dependent Riccati equation method*. International Journal of robust and nonlinear control; 1998; 8: pp. 401-433.

Nozaki, R., Balthazar, J.M., Tusset, A.M., Bueno, A.M., Pontes,. B.R. *Nonlinear Control System Applied to Atomic Force Microscope Including Parametric Errors.* Journal of Control, Automation and Electrical Systems. DOI: 10.1007/s40313-013-0034-1

Nayfeh, AH. *Introduction to Perturbation Techniques*. Wiley, New York. 1981.

Packard, N., Crutchfield, J., Farmer, D., Shaw, R. (1980). *Geometry from a time series*. Physical Review Letters 45:712-715

Payam, AF., Fathipour M, Yazdanpanah MJ. *High precision imaging for non-contact mode atomic force microscope using an adaptive nonlinear observer and output state feedback controller.* Digest Journal of Nanomaterials and Biostructures; 2009; 4(3): pp. 429-442.

Piccirillo, V., Balthazar JM, Pontes BR., Felix JLP. *Chaos control of a nonlinear oscillator with shape memory alloy using an optimal linear control: Part I: Ideal energy source*. Nonlinear Dynamics; 2009; 55 (1-2): pp.139-149.

Piccirillo, V., Balthazar, J.M., Pontes, B.R., Felix, J.L.P.: *Chaos control of a nonlinear oscillator with shape memory alloy using an optimal linear control: Part II: Non-Ideal energy source*. Nonlinear Dynamics, 2009; 56 (3): pp. 243-253.

Rafikov, M, Balthazar JM. *On control and synchronization in chaotic and hyperchaotic systems*. Communications in Nonlinear Science & Numerical Simulation; 2008; 13: pp. 1246-1255.

Rafikov, M., Balthazar JM., Tusset. AM. *An Optimal Linear Control Design for Nonlinear Systems*. J. of the Braz. Soc. of Mech. Sci. & Eng.; 2008; XXX(4): pp. 279:284.

Rafikov, M., Balthazar, J. M.: *On an optimal control design for Rössler system*. Phys. Lett. A, 2004; 333: pp. 241-245.

Raman, A., Melcher J, Tung R. *Cantilever Dynamics in Atomic Force Microscope. Nanotoday*; 2008; 3, 1-2: pp. 20-27.

Ricardo, G. San Paulo A. *Dynamics of a vibrating tip near or in intermittent contact with a surface*. Physical Review B; 2000; 61, 20.

Rodrigues, KS., Balthazar JM., Tusset AM., Pontes Jr BR. *On a control design to an AMF microcantilever beam, operating in a tapping mode, with irregular behavior.* ASME 2011, Washington. International Design Engineering Technical Conferences (IDETC) and Computers and Information in Engineering Conference (CIE); 2011.

Sader, J. E., Chon, J. W. M., and Mulvaney, P., *Calibration of rectangular atomic force microscope cantilevers*. Rev. Sci. Instrum., 70, 3967 (1999)

Salarieh, V., Alasty A. *Control of chaos in atomic force microscopes using delayed feedback based on entropy minimization*. Communications in Nonlinear Science and Numerical Simulation; 2009; 14: pp. 637-644.

Sebastian, R, Lee SL, Raman A. *Nonlinear dynamics of atomic-force-microscope probes driven in Lennard -Jones potentials*. Proc. R. Soc. Lond.; 2003; 459: pp. 1925-1948.

Shawky, AM, Ordys AW, Petropoulakis L, Grimble MJ. *Position control of flexible manipulator using non-linear with state-dependent Riccati equation*. J. Systems and Control Engineering; 2007; pp. 475-486.

Sinha, A. *Nonlinear dynamics of atomic force microscope with PI feedback. Journal of Sound and Vibration*; 2005; 288: pp.387-394.

Takens, F. (1981) *Detecting strange attractors in turbulence*. Lecture Notes in Mathematics 898, Berlin:Springer-Verlag

Tusset, AM., Balthazar, J.M., Chavarette, FR, Felix, J.L.P.: *On energy transfer phenomena, in a nonlinear ideal and nonideal essential vibrating systems, coupled to a (MR) magneto-rheological damper.* Nonlinear Dynamics, 2012: pp. 1-22.

Tusset, AM., Balthazar, J.M., Chavarette, FR, Felix, J.L.P.: *Statements on chaos control designs, including a fractional order dynamical system, applied to a "MEMS" comb-drive actuator*. Nonlinear Dynamics, 2012: pp. 1-21.

Tusset, AM., Balthazar, J.M., Felix, J.L.P.: *On elimination of chaotic behavior in a non-ideal portal frame structural system, using both passive and active controls*. Nonlinear Dynamics, 2012: pp. 1-11.

Tusset, AM., Rafikov, M., Balthazar, JM. *An Intelligent Controller Design for Magnetorheological Damper Based on a Quarter-car Model*. Journal of Vibration and Control; 2009 15 (12): pp. 1907-1920.

Wang, CC, Paib NS, Yauc HTl. *Chaos control in AFM system using sliding mode control by backstepping design*. Communications in Nonlinear Science Numerical Simulation; 2009.

Yabuno, H. *Stabilization and utilization of nonlinear phenomena based on bifurcation control for slow dynamics*. Journal of Sound and Vibration; 2008; 315: pp. 766-780.

Yabuno, H., Kaneko H., Kuroda M., Kobayashi T. *Van der Pol type self-excited micro-cantilever probe of atomic force microscopy*. Nonlinear Dyn.; 2008; 54: pp. 137-149.

Yamasue, K., Hikihara T. *Control of microcantilevers in dynamic force microscopy using time delayed feedback.* Review of Scientific Instruments; 2006; 77, 053703: pp. 1-6.

Zhang, WM, Meng G, Zhou JB, Chen JY, *Nonlinear Dynamics and Chaos of Microcantilever-Based TM-AFMs with Squeeze Film Damping Effects*. Sensors; 2009, pp. 3854-3874.

7. RESPONSIBILITY NOTICE

The author(s) Ricardo Nozaki, José Manoel Balthazar, Angelo Marcelo Tusset, Atila Bueno Madureira, Bento Pontes Rodrigues Jr., and Helio Aparecido Navarro are the only responsible for the printed material included in this paper.